Int. J. Solids Structures Vol. 17, pp. 811-825, 1981
Printed in Great Britain

0020-7683/81/080811-15$02.00/0
Pergamon Press Ltd.

NONLINEAR AXISYMMETRIC BENDING OF ANNULAR PLATES WITH VARYING THICKNESS

J. N. Reddy
Department of Engineering Science and Mechanics, Virginia Polytechnic Institute and State University, Blacksburg, VA, 24061 U.S.A.

and

C. L. Huang
School of Aerospace, Mechanical, and Nuclear Engineering, University of Oklahoma, Norman, OK 73019, U.S.A.

(*Received* 14 *July* 1980; *in revised form* 6 *November* 1980)

Abstract—Finite-element analysis of the large deflection bending of annular plates with variable thickness is presented. The more general Reissner plate equations as well as von Karman plate equations are used in the formulation. Stresses and deformation results are presented showing the effects of radius-to-thickness ratio (i.e. shear deformation), nonlinearity and material orthotropy. The finite-element solutions are found to be in good agreement with available exact and approximate analytical solutions.

INTRODUCTION

Annular plate is employed in machine design as a coupling for power transmission shafts which, due to bending and thermal expansion, may become misaligned. Such a coupling has no moving parts and has a longer life expectancy. Maximum stresses in annular plates can be controlled by design of the plate thickness profile. Circular plates of non-uniform thickness are also encountered in the design of diaphragms of steam turbines, piston heads and cylinder heads. Plates such as the flexible diaphragm coupler have been designed to transmit torque while sustaining transverse deflections that are several times their minimum thickness. Consequently, the geometric nonlinearity must be accounted for in the response analysis. Further, the low ratio of radius-to-thickness (minimum) of the plate requires inclusion of the transverse shear strain in the analysis. The use of anisotropic and composite materials provides the designer with an added flexibility of tailoring the material property to a greater advantage. However, inclusion of the geometric nonlinearity and thickness shear results in the stress analysis of more complex problems involving anisotropic plates.

For plates made of isotropic materials, there exist design data, based on linear analyses, both in the case of uniform thickness[1-10] and variable thickness[11-25]. Conway's[12] paper contains design data for axisymmetric bending of annular plates with linearly varying thickness. Similar data for symmetric and asymmetric (skew) bending of annular plates with a power law thickness profile is given in a comprehensive paper by Wolff[17]; however, these investigations were based on the classical (i.e. Kirchoff) plate theory and did not account for the transverse shear strains. Mindlin and Deresiewicz[2, 3], Lehnhoff *et al.*[5, 6] and Bapu Rao and Kumaran[11] have studied the influence of transverse shear on the bending of circular plates; however, the study was limited to uniform thickness plates. Pardoen[9] reported finite-element results for the axisymmetric bending of uniform thickness circular plates, while Bapu Rao and Kumaran[11] presented a finite-element displacement formulation with shear deformation for axisymmetric bending of uniform thickness annular plates. Finite element bending and free vibration analyses of variable thickness plates have been performed, without including the transverse shear strains, by Wilson and Kirkhope[22, 23] and Irie *et al.*[24, 25].

Bending of anisotropic plates of constant thickness under lateral loads and the buckling analysis under inplane loads have been studied by Carrier[26, 27]. Sherbourne and Murthy[28, 29] presented analytical results for bending of cylindrically orthropic circular plates of variable thickness. These studies were based on the classical plate theory and did not account for shear deformation and large deflections.

Nonlinear analysis of bending of a wide range of annular plates of uniform thickness was performed by Hart and Evans[30] for symmetric bending and by Alzheimer and Davis[31] for unsymmetrical bending. In [30] analytical solutions to the Reissner plate equations as well as the von Karman plate equations were obtained. Tielking[32, 33] employed the potential energy formulation of von Karman plate theory and the Ritz method to obtain the stress and deformation solutions for symmetric as well as unsymmetric bending of variable thickness annular plates with built-in edges. However, the study did not include the transverse shear strains. Nonlinear vibrations of circular plates have been investigated by Wah[34], and Ramachandran[35].

Despite many approximate, analytical investigations, only a few finite-element analyses of nonlinear bending and vibration of annular plates are reported in the literature, and all of them are devoted to vibrations of uniform thickness plates (see[36–39]). With the advent of the digital computer and the finite element method, variable thickness plates can be analyzed for arbitrary thickness profiles. The present study was undertaken to exploit the potential of the finite element method to nonlinear bending and vibration of orthotropic annular plates with variable thickness.

GOVERNING EQUATIONS AND VARIATIONAL FORMULATIONS

Governing equations

Consider an annular plate of thickness t, outside radius b, and internal radius a. The coordinate system was chosen such that the middle plane, R, of the plate coincides with the $r-\theta$ plane, the origin of the coordinate system being at the center of the plate with the z-axis upward. The thickness t is assumed to be a function of the radius, $t = t(r)$, the form of which will be given during the discussion of numerical results.

The displacement field in the shear deformable (i.e. Reissner–Mindlin) theory of axisymmetric circular plates is given by,

$$u_r(r, z) = u_0(r) + z\psi(r), \tag{1}$$

$$u_\theta = 0, \quad u_z = w(r),$$

where u_0 is the in-plane displacement of the midplane, u_r, u_θ and u_z are the displacements along r, θ and z directions, respectively and ψ is the shear rotation. For classical (thin) plate theory, one assumes

$$\psi = -\frac{\mathrm{d}w}{\mathrm{d}r}. \tag{2}$$

Indeed, one can construct the shear deformable theory of plates treating eqn (2) as a constraint and then using the so-called penalty method to include the constraint in the variational formulation of the classical plate theory. A penalty-formulation and its relation to the displacement type models and mixed models of plates are illustrated in [40, 41].

The strain-displacement equations of the large displacement theory (in the von Karman sense) are given by

$$\epsilon_r = \frac{\partial u_r}{\partial r} + \frac{1}{2}\left(\frac{\partial w}{\partial r}\right)^2 = \frac{\mathrm{d}u_0}{\mathrm{d}r} + z\frac{\mathrm{d}\psi}{\mathrm{d}r} + \frac{1}{2}\left(\frac{\mathrm{d}w}{\mathrm{d}r}\right)^2,$$

$$\epsilon_\theta = \frac{1}{r}\frac{\partial u_\theta}{\partial \theta} + \frac{u_r}{r} + \frac{1}{2}\left(\frac{1}{r}\frac{\partial u_r}{\partial \theta}\right)^2 = \frac{u_0 + z\psi}{r},$$

$$\epsilon_{zz} = \frac{\partial u_z}{\partial z} = 0, \quad 2\epsilon_{r\theta} = \frac{\partial u_\theta}{\partial r} + \frac{1}{r}\frac{\partial u_r}{\partial \theta} - \frac{u_\theta}{r} + \frac{1}{r}\frac{\partial u_z}{\partial \theta}\frac{\partial u_z}{\partial r} = 0, \tag{3}$$

$$\epsilon_{rz} = \frac{1}{2}\left(\frac{\partial u_r}{\partial z} + \frac{\partial u_z}{\partial r}\right) + \frac{1}{2}\frac{\partial u_z}{\partial r}\frac{\partial u_z}{\partial z} = \frac{1}{2}\left(\psi + \frac{\mathrm{d}w}{\mathrm{d}r}\right).$$

The equilibrium equations of the theory (for the axisymmetric case) are given by

$$
\begin{aligned}
&-\frac{\mathrm{d}}{\mathrm{d}r}(rN_r)+N_\theta=0,\\
&-\frac{\mathrm{d}}{\mathrm{d}r}\left(r\frac{\mathrm{d}w}{\mathrm{d}r}N_r\right)-\frac{\mathrm{d}}{\mathrm{d}r}(rQ)=qr, \qquad (4)\\
&-\frac{\mathrm{d}}{\mathrm{d}r}(rM_r)+M_\theta+Qr=0,
\end{aligned}
$$

where N_r and N_θ are the stress resultants, M_r and M_θ the stress couples and Q is the transverse shear resultant,

$$
\begin{aligned}
(N_r, N_\theta)&=\int_{-t/2}^{t/2}(\tau_r, \tau_\theta)\,\mathrm{d}z,\\
(M_r, M_\theta)&=\int_{-t/2}^{t/2}(\tau_r, \tau_\theta)z\,\mathrm{d}z, \qquad (5)\\
Q&=\int_{-t/2}^{t/2}\tau_{rz}\,\mathrm{d}z.
\end{aligned}
$$

Here τ_r, τ_θ and τ_{rz} are the in-plane stresses.

Assuming elastic behavior, the constitutive equations of the theory can be expressed in the form,

$$
\begin{aligned}
\tau_r&=c_{11}\epsilon_r+c_{12}\epsilon_\theta,\\
\tau_\theta&=c_{12}\epsilon_r+c_{22}\epsilon_\theta, \qquad (6)\\
\tau_{rz}&=2c_{33}\epsilon_{rz},
\end{aligned}
$$

where c_{ij} are the elastic coefficients.

Substituting eqns (3) and (6) into eqn (5), we obtain

$$
\begin{aligned}
N_r&=A_{11}\left[\frac{\mathrm{d}u_0}{\mathrm{d}r}+\frac{1}{2}\left(\frac{\mathrm{d}w}{\mathrm{d}r}\right)^2\right]+A_{12}\frac{u_0}{r},\\
N_\theta&=A_{12}\left[\frac{\mathrm{d}u_0}{\mathrm{d}r}+\frac{1}{2}\left(\frac{\mathrm{d}w}{\mathrm{d}r}\right)^2\right]+A_{22}\frac{u_0}{r},\\
M_r&=D_{11}\frac{\mathrm{d}\psi}{\mathrm{d}r}+D_{12}\frac{\psi}{r}, \qquad (7)\\
M_\theta&=D_{12}\frac{\mathrm{d}\psi}{\mathrm{d}r}+D_{12}\frac{\psi}{r},\\
Q&=A_{33}\left(\psi+\frac{\mathrm{d}w}{\mathrm{d}r}\right),
\end{aligned}
$$

where the A_{ij} and D_{ij} are the stiffness coefficients defined by

$$
(A_{ij}, D_{ij})=\int_{-t/2}^{t/2}c_{ij}(1, z^2)\,\mathrm{d}z, \quad (i, j=1, 2, 3), \qquad (8)
$$

and $A_{33}=2ktc_{33}$. Note that the stiffness coefficients are functions of the position, r, in a variable-thickness plate. Here k denotes the shear correction factor.

Variational formulation

The conventional formulation is based on the total potential energy functional expressed in terms of the generalized displacements, u_0, w and ψ. The variational (or weak) form associated with eqns (4), expressed in terms of the displacements, is given by

$$\delta\pi = \delta(U+V) = 2\pi\int_a^b \left\{\left[A_{11}\left(\frac{\mathrm{d}u_0}{\mathrm{d}r}+\frac{1}{2}\left(\frac{\mathrm{d}w}{\mathrm{d}r}\right)^2\right)+A_{12}\frac{u_0}{r}\right]\left(\frac{\mathrm{d}\delta u_0}{\mathrm{d}r}+\frac{\mathrm{d}w}{\mathrm{d}r}\frac{\mathrm{d}\delta w}{\mathrm{d}r}\right)\right.$$

$$+\frac{1}{r}\left[A_{12}\left(\frac{\mathrm{d}u_0}{\mathrm{d}r}+\frac{1}{2}\left(\frac{\mathrm{d}w^2}{\mathrm{d}r}\right)^2\right)+A_{22}\frac{u_0}{r}\right]\delta u_0$$

$$+\left(D_{11}\frac{\mathrm{d}\psi}{\mathrm{d}r}+D_{12}\frac{\psi}{r}\right)\frac{\mathrm{d}\delta\psi}{\mathrm{d}r}+\frac{1}{r}\left(D_{12}\frac{\mathrm{d}\psi}{\mathrm{d}r}+D_{22}\frac{\psi}{r}\right)\delta\psi$$

$$\left.+A_{33}\left(\psi+\frac{\mathrm{d}w}{\mathrm{d}r}\right)\left(\delta\psi+\frac{\mathrm{d}\delta w}{\mathrm{d}r}\right)\right\}r\,\mathrm{d}r-2\pi\int_a^b qr\delta w\,\mathrm{d}r \tag{9}$$

where q is the distributed transverse loading.

One can obtain the formulations associated with the large deflection theory of thin plates (i.e. not including the shear deformation effects) from eqn (9) by replacing ψ by $-(\mathrm{d}w/\mathrm{d}r)$ (see eqn (2)).

FINITE ELEMENT MODELS

Here we present a finite element model based on the functional in (9). We assume that the variables u_0, w and ψ are interpolated by expressions of the form

$$u_0=\sum_i u_iN_i,\quad w=\sum_i w_iN_i,\quad \psi=\sum_i \psi_iN_i,\quad \text{etc.} \tag{10}$$

where N_i the finite element interpolation functions. Substituting eqn (10) into eqn (9), we obtain

$$\begin{bmatrix} 2[K^{11}] & [K^{12}] & [0] \\ & [K^{22}] & [K^{23}] \\ \text{symm.} & & [K^{33}] \end{bmatrix}\begin{Bmatrix}\{u\}\\\{w\}\\\{\psi\}\end{Bmatrix}=\begin{Bmatrix}\{0\}\\\{F\}\\\{0\}\end{Bmatrix}. \tag{11}$$

In the case of free vibration, the above equation takes the form,

$$([K]-\rho\omega^2[M])\{\Delta\}=\{0\}, \tag{12}$$

where ω is the natural frequency of vibration. The stiffness coefficients $K_{ij}^{\alpha\beta}$, and mass coefficients, $M_{ij}^{\alpha\beta}$ are given by

$$K_{ij}^{11}=A_{11}R_{ij}^{11}+A_{12}(S_{ij}^{01}+S_{ij}^{10})+A_{22}\int_0^h \frac{1}{r}N_iN_j\,\mathrm{d}r$$

$$K_{ij}^{12}=A_{11}\int_0^h\left(\frac{\mathrm{d}w}{\mathrm{d}r}\right)N_{i,r}N_{j,r}r\mathrm{d}r+A_{12}\int_0^h\left(\frac{\mathrm{d}w}{\mathrm{d}r}\right)N_iN_{j,r}\,\mathrm{d}r$$

$$K_{ij}^{22}=A_{11}\int_0^h\frac{1}{2}\left(\frac{\mathrm{d}w}{\mathrm{d}r}\right)^2 rN_{i,r}N_{j,r}\,\mathrm{d}r+A_{33}R_{ij}^{11} \tag{13}$$

$$K_{ij}^{23}=A_{33}R_{ij}^{10},\quad \bar{K}_{ij}^{33}=A_{33}R_{ij}^{00}$$

$$K_{ij}^{33}-A_{33}R_{ij}^{00}+D_{11}R_{ij}^{11}+D_{12}(S_{ij}^{01}+S_{ij}^{10})+D_{22}\int_0^h\frac{1}{r}N_iN_j\,\mathrm{d}r$$

$$M_{ij}^{\alpha\beta}=0\ \text{for}\ \alpha\neq\beta,\quad M_{ij}^{\alpha\alpha}=R_{ij}^{00},\quad F_i=\int_0^h qN_ir\,\mathrm{d}r, \tag{14}$$

$$S_{ij}^{mn}=\int_0^h\frac{\mathrm{d}^mN_i}{\mathrm{d}r^m}\frac{\mathrm{d}^nN_j}{\mathrm{d}r^n}\mathrm{d}r,\quad R_{ij}^{mn}=\int_0^h\frac{\mathrm{d}^mN_i}{\mathrm{d}r^m}\frac{\mathrm{d}^nN_j}{\mathrm{d}r^n}r\mathrm{d}r,\quad (m,n=0,1,2). \tag{15}$$

Various other special models can be developed from eqn (9). For example, the conventional model associated with the thin theory is given by (setting $\psi = -\mathrm{d}w/\mathrm{d}r$ in eqn (9)),

$$\begin{bmatrix} 2[K^{11}] & [K^{12}] \\ [K^{12}]^T & [\bar{K}^{22}] \end{bmatrix} \begin{Bmatrix} \{u\} \\ \{w\} \end{Bmatrix} = \begin{Bmatrix} \{0\} \\ \{F\} \end{Bmatrix}, \tag{16}$$

where

$$\bar{K}_{ij}^{22} = A_{11}\int_0^h \left[\frac{1}{2}\left(\frac{\mathrm{d}w}{\mathrm{d}r}\right)^2\right] N_{i,r}N_{j,r}r\,\mathrm{d}r + D_{22}\int_0^h \frac{1}{r}N_iN_j\,\mathrm{d}r + D_{11}R_{ij}^{22} + D_{12}(S_{ij}^{12} + S_{ij}^{21}). \tag{17}$$

Note that the stiffness coefficients $\bar{K}_{ij}^{22}$ contain the second derivatives of the interpolation functions N_i, and therefore the transverse deflection w must be approximated by cubic polynomials, as in the conventional formulation of thin beams (see e.g. Reddy *et al.*[42, 43]).

NUMERICAL RESULTS

In this section, we shall present only representative results for circular and annular plates under various edge conditions and loadings. Numerical results are presented to show relative accuracy of the various models in comparison to the results of other investigations and exact solutions (for linear case), and to show the effects of shear deformation and nonlinearity on the deflections, moment resultants and frequencies.

Static bending analysis results

The plate thickness profile is assumed to be of the form

$$t(r) = t_0\left(\frac{r}{b}\right)^{-k/3} \tag{18}$$

where t_0 is the plate thickness at the outer edge ($r = b$) and k is a real number whose value dictates the form of the profile. For example, the diaphragm coupler is designed with a "hyperbolic" profile which is obtained by setting $k = 3$ in eqn (18).

First, the results of linear analyses are presented. Table 1 shows the nondimensionalized maximum deflections (w) and maximum stresses (σ_r) for simply-supported orthotropic annular plates subjected to uniform pressure loading (P). The finite-element solutions are compared with the small-deflection, classical plate theory (CPT) (i.e. without shear deformation) results of Sherbourne and Murthy[28]. As can be seen the finite-element results are in close agreement with the analytical solution[28]. With increasing ratio of a to b, the plate becomes more flexible and therefore deflects more (for a fixed radius, b). The finite-element results corresponding to the shear deformation theory (SDT) are also listed in the same table. As expected, the deflections are slightly larger than those obtained by the classical theory. Note that a converging plate (i.e. tapered down toward the center) with a positive value of k has lower displacements and stresses compared to a negative value of k. It can be seen from the table that the maximum stress for $k = -1$ is 6.27 times larger than the maximum stress for $k = 1$, and the displacement is about 5.2 times larger. Similar results are presented in Table 2 for the same material-plates with clamped boundary condition and point load (P_0) at the center. Figure 1 shows the influence of taper on the surface stress distribution in a clamped annular plate with hub thickness $t_a = 0.039$ in. (1.0 mm) and radii $a = 1.0$ (25.4 mm), $b = 2.0$ (50.8 mm). This is the same problem considered by Tielking[32]. The results are in good agreement, visually, with those in[32].

Next, the effect of shear deformation on the deflections of simply supported isotropic plate under uniform loading and clamped isotropic plate under point load are shown, respectively, in Figs. 2 and 3. The solutions were obtained using 20 elements. Figure 4 shows the effect of radius-to-thickness ratio on the nondimensionalized maximum deflection of clamped, orthotropic, annular plate under concentrated load at the center. For radius-to-thickness values smaller

Table 1. Nondimensionalized deflections and stresses simply supported, orthotropic, variable-thickness† annular plate under uniform loading ($E_2/E_1 = 0.5625$, $\nu_{12} = 0.5925$, $b/t = 10$)

a/b	k	$\lambda \times 10^2$			$\mu \times 10^2$		
		Ref.[28]	Present		Ref.[28]	Present	
			CPT	SDT		CPT	SDT
0.2	3	6.518	6.518	7.110	38.855	39.037 (.6828)*	38.985 (.6716)*
	1	24.326	24.325	25.057	79.368	79.641 (.3628)	79.618 (.3516)
	0	54.348	54.345	55.170	205.40	202.74 (.2028)	199.88 (.2085)
	-1	127.88	127.87	128.81	498.00	484.05 (.2028)	471.40 (.2085)
0.3	3	5.684	5.684	6.202	36.071	36.166 (.6874)	36.124 (.6776)
	1	18.226	18.225	18.847	73.245	73.271 (.3466)	73.271 (.3424)
0.4	3	4.485	4.485	4.913	32.191	32.215 (.6979)	32.196 (.6937)
	1	12.122	12.121	12.620	63.063	62.982 (.4321)	63.062 (.4063)
0.5	3	3.092	3.092	3.422	27.201	27.223 (.7017)	27.222 (.7053)
	1	6.999	6.999	7.374	49.844	49.852 (.5017)	49.842 (.5063)

$\lambda = wD/Pb^4$, $\mu = \sigma_{max}\, t_0^2/Pb^2$, $D = E_1 t_0^3/12(1-\nu_{21}\nu_{12})$

* Gauss point

† thickness, $t = t_0(r/b)^{-k/3}$.

Table 2. Nondimensionalized deflections and stresses for clamped, orthotropic, variable-thickness annular plate under point load ($E_2/E_1 = 0.5625$, $\nu = 0.5925$, $b/t = 10$)

a/b	k†	$\lambda \times 10^2$			$\mu \times 10^2$		
		Ref.[28]	Present		Ref.[28]	Present	
			CPT	SDT		CPT	SDT
0.2	3	1.538	1.538	2.037	-21.279	-20.899 (.9972)*	-18.888 (.9800)*
	1	5.672	5.672	6.444	52.467	51.953 (.2028)	49.373 (.2200)
	0	11.501	11.500	12.471	123.54	120.29 (.2028)	107.55 (.2200)
	-1	22.994	22.990	--	268.83	255.71 (.2028)	--
0.3	3	1.378	1.378	1.815	-20.770	-20.443 (.9976)	-18.681 (.9825)
	1	4.067	4.066	4.682	44.169	43.803 (.3024)	42.732 (.3175)
0.4	3	1.122	1.121	1.497	-19.713	-19.439 (.9979)	-17.936 (.9850)
	1	2.674	2.674	3.165	36.245	35.968 (.4021)	34.324 (.4150)
	0	4.123	4.123	4.689	58.261	57.476 (.4021)	53.417 (.4150)
0.5	3	1.378	1.378	1.815	-20.770	-20.443 (.9976)	-18.681 (.9825)
	1	4.067	4.066	4.682	44.169	43.803 (.3024)	41.732 (.3175)

$\lambda = wD/P_0 b^2$, $\mu = \sigma_{max}\, t_0^2/P_0$, $D = E_1 t_0^3/12(1-\nu_{21}\nu_{12})$

* Gauss point

† see Table 1 for the thickness variation

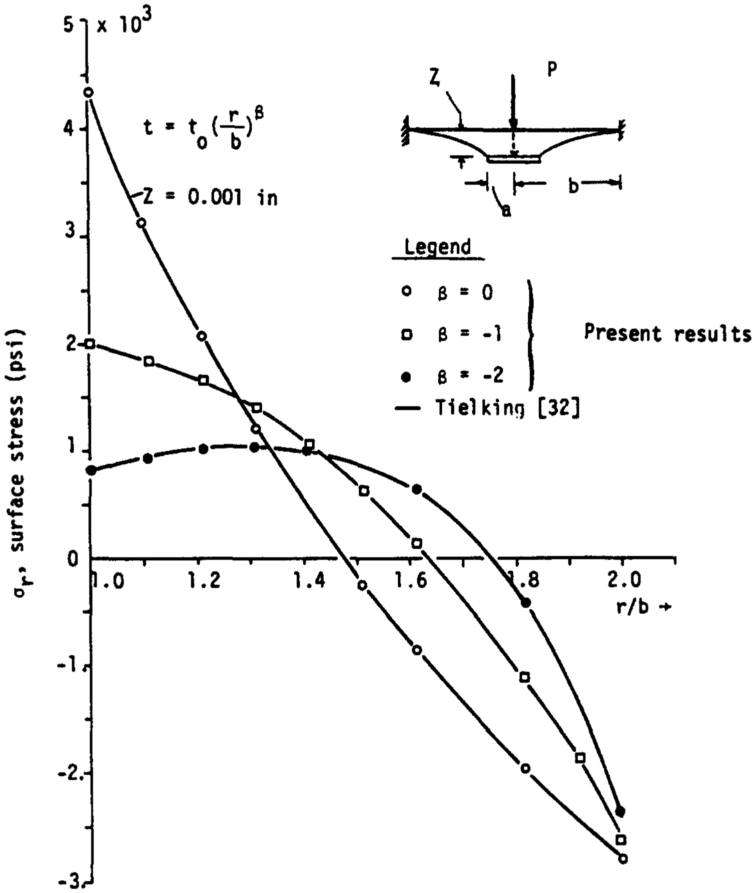

Fig. 1. The influence of taper on the surface stress distribution in a clamped annular plate under point load at the center ($a/b = 0.5$, Material 2).

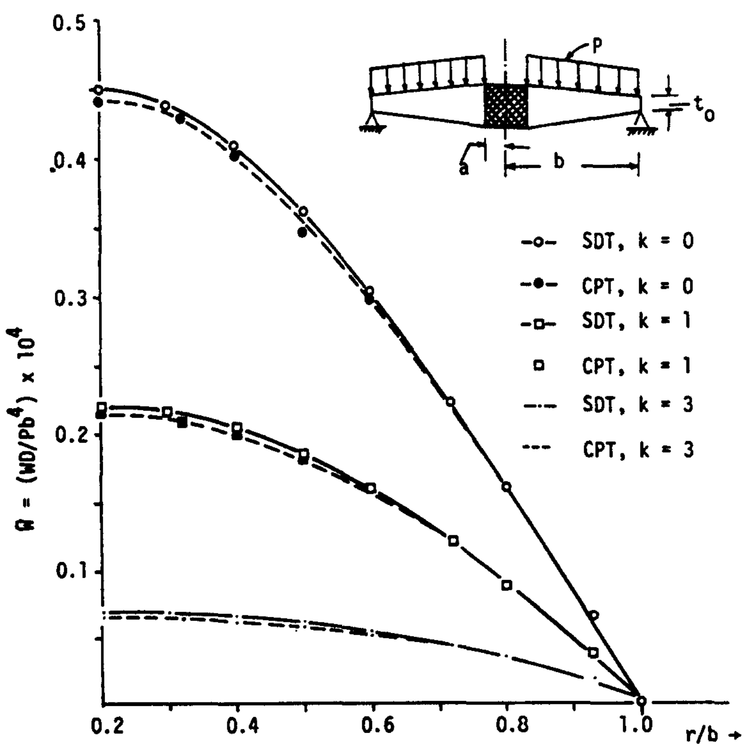

Fig. 2. Nondimensionalized deflections obtained by thin and thick-plate theories for isotropic ($\nu = 1/3$) simply supported, annular plates under uniform loading ($b/a = 5$, $b/t_0 = 10$).

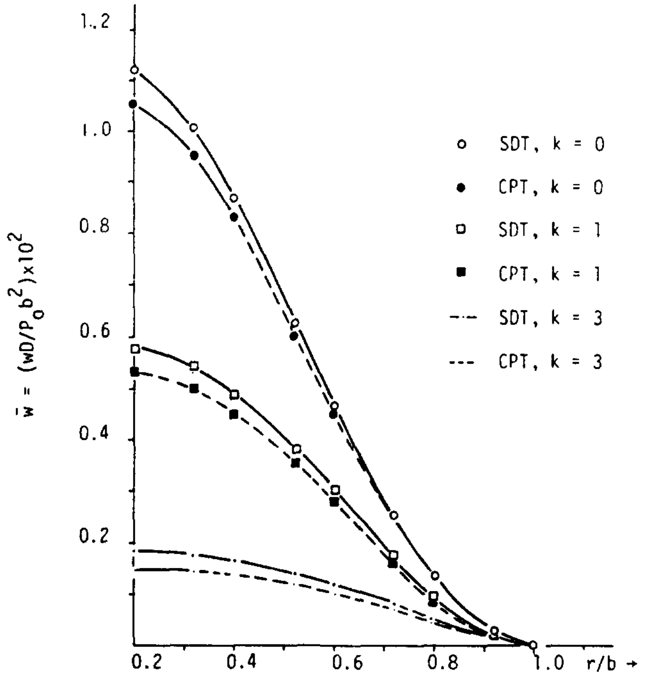

Fig. 3. Comparison of the nondimensionalized deflections obtained by thin-and thick-plate theories for isotropic ($\nu = 1/3$) clamped annular plates under point load at the center ($b/a = 5$, $b/t_0 = 10$).

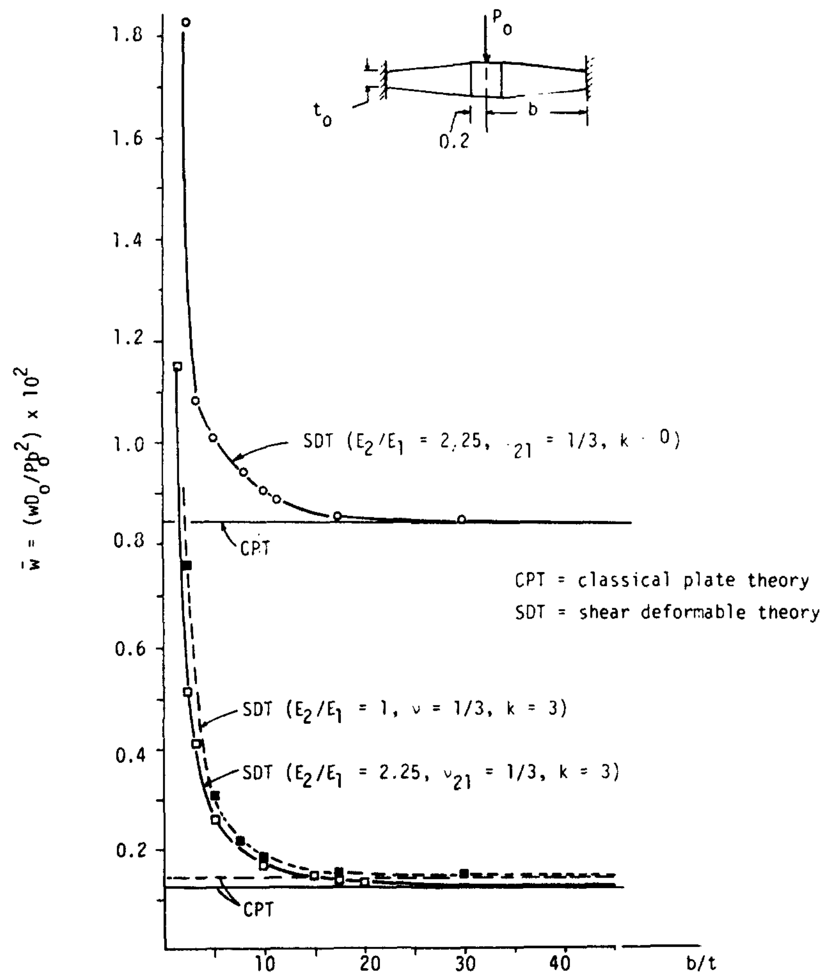

Fig. 4. Effect of radius-to-thickness ratio on the nondimensionalized deflection of clamped orthotropic annular plates under point load at the center ($b/a = 5$).

than 20, the deflection is sensitive to the inclusion of the transverse shear strains in the analysis.

The results of nonlinear analyses are discussed next. The influence of large deflections, z (specified), on the surface stress distribution in a clamped plate with hyperbolid taper, $\beta = -2$ (see [32]) is shown in Fig. 5. The results were obtained using the classical plate thoery. The solutions are in close agreement with those presented in [32]. Figure 6 shows the stress (σ_r) distribution as a function of r for a simply supported isotropic annular plate under various intensities of uniform loading (P). The solution was obtained using 10 CPT elements in the half plate. Finally, Figs. 7 and 8 show the nondimensionalized load-deflection and load-stress curves for simply supported annular plates under uniform loading, and clamped annular plates under point load at the center, respectively. Again, the deflections obtained using shear deformation results are larger than the corresponding results obtained by using the thin plate theory.

Free vibration analysis results

Numerical results are presented for variable thickness circular plates with simply-supported and clamped boundary conditions. Classical as well as shear deformable theories were used in the analysis.

First a comparison is made of the present finite element results with the exact solution and with those obtained by Irie *et al.*[25] using transfer matrix method. The shear deformable theory was used in both investigations; however, the large deflection effects were not accounted

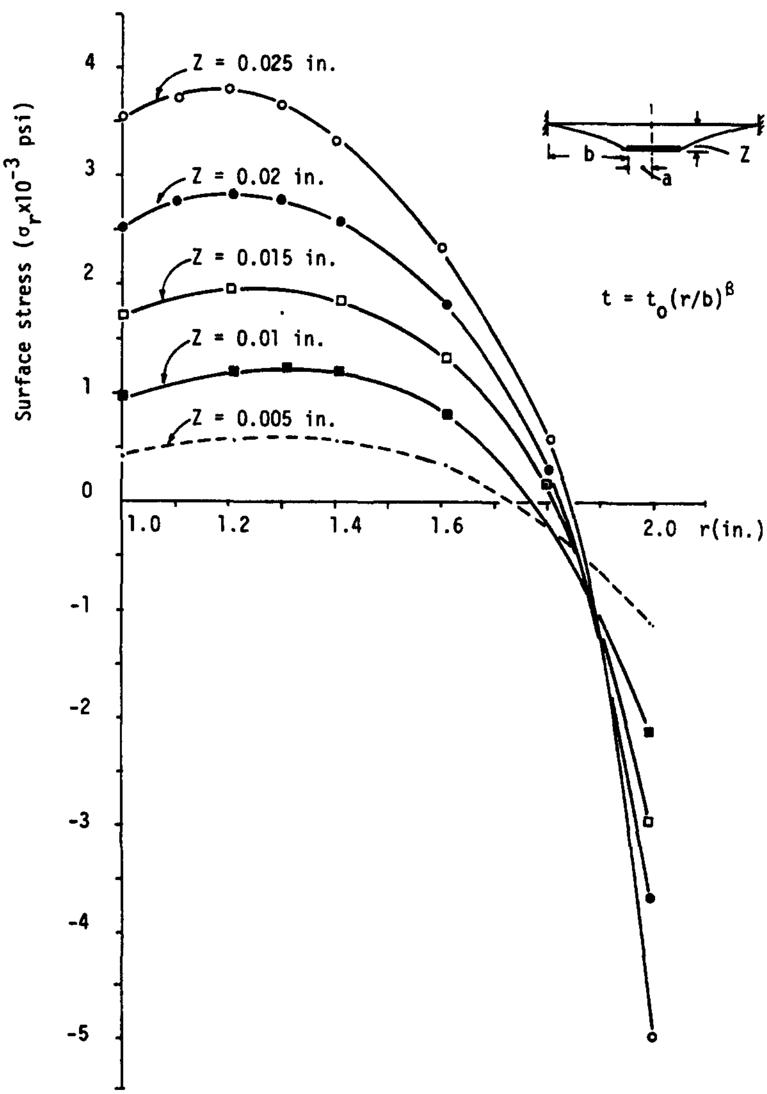

Fig. 5. The influence of large deflections on the surface stress distribution in a clamped plate with hyperbolic taper ($\beta = -2$).

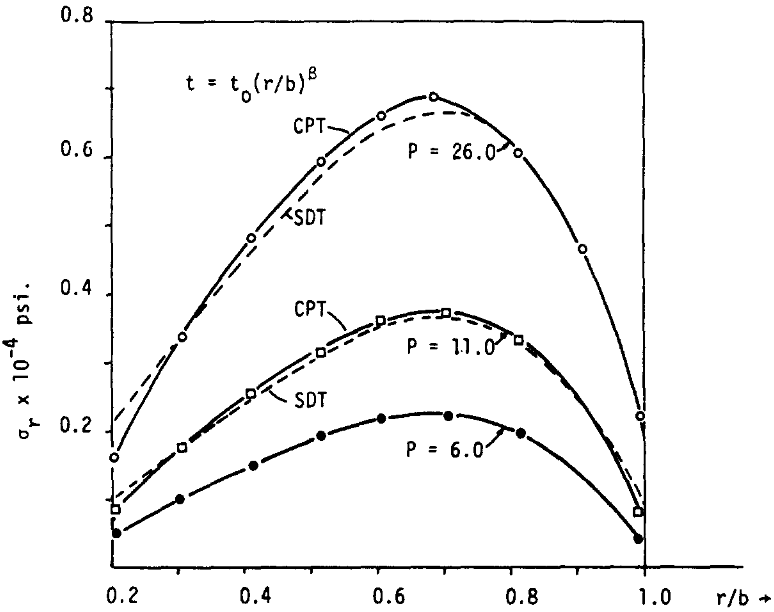

Fig. 6. Influence of large deflections on the surface stress distribution in a simply supported isotropic plate ($\nu = 1/3$) with hyperbolic taper ($\beta = -2$).

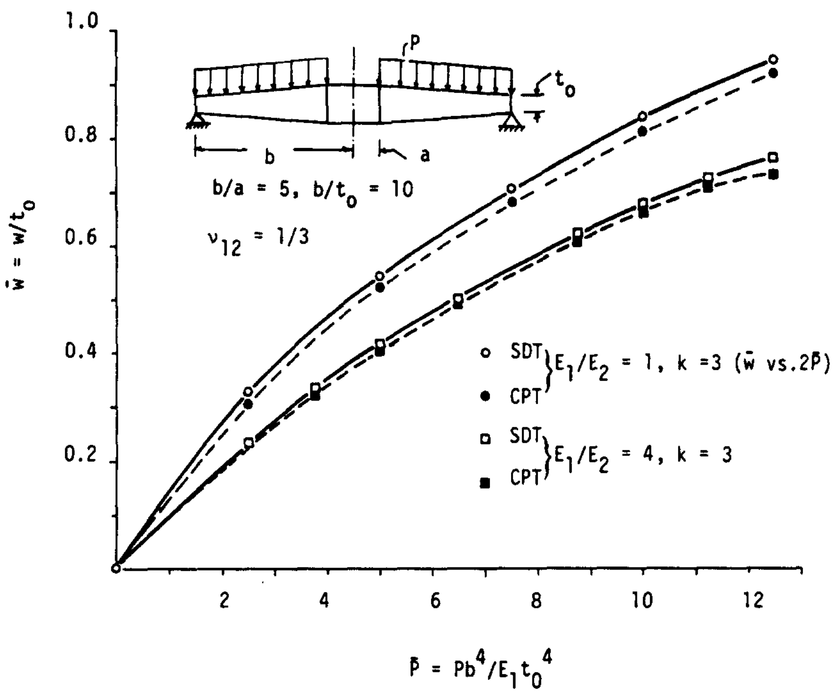

Fig. 7. Load-deflection curves for simply supported annular plates under distributed loading ($b/a = 5$, $b/t_0 = 10$).

for in [25]. The thickness is assumed to vary according to

$$t = t_0 - (t_0 - t_1)\left(\frac{r-a}{b-a}\right)^m, \quad m > 0 \tag{19}$$

where t_0 is the thickness of the outer rim and t_1 is the thickness of the inner rim. Table 3 shows a comparison of nondimensionalized fundamental frequency obtained by various investigators for free-clamped annular plates of uniform thickness ($E_2/E_1 = 1$, $\nu = 0.3$, $m = 0$). Table 4 presents similar results for free-clamped annular plates of linearly varying thickness ($m = 1$).

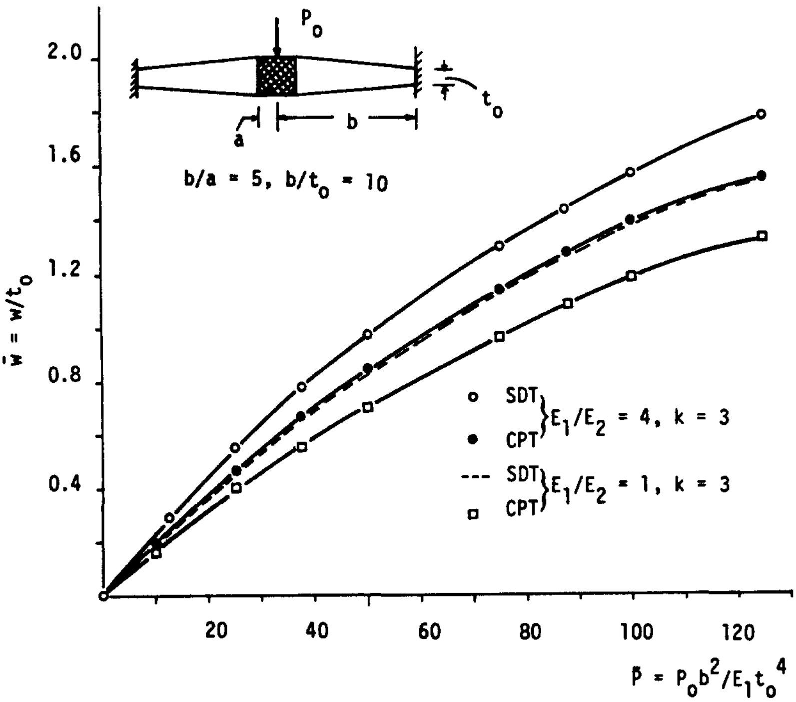

Fig. 8. Load-deflection curves for clamped annular plates under point load at the center ($b/a = 5$, $b/t_0 = 10$).

Table 3. Comparison of nondimensionalized fundamental frequency (λ)* of free-clamped annular plates of uniform thickness† ($m = 0$, $E_1/E_2 = 1$, $\nu = 0.3$)

$\frac{a}{b}$	$\frac{b}{t_0}$	Present FEM	Exact [2]	Rao and Prasad [10]	Spline Technique [24]	Transfer Matrix [25]
0.3	5	2.477	2.477	2.543	2.479	2.477
	2	2.150	2.148	2.546	2.148	2.148
0.5	5	3.387	3.385	3.151	3.385	3.385
	2	2.809	2.805	3.541	2.805	2.805

* $\lambda = \omega^2\rho t_0 b^4/D$; † thickness as given in eqn (19).

Table 4. Comparison of nondimensionalized fundamental frequency (λ) of free-clamped annular plates of linearly varying thickness† ($m = 1$, $E_1/E_2 = 1.0$, $\nu = 0.3$, $A/B = 0.1$)

t_1/t_0	Shear deformable theory (SDT)						classical (CPT)
	$t_0/b=0.1$		$t_0/b=0.2$		$t_0/b=0.3$		
	present	Ref.[25]	present	Ref.[25]	present	Ref.[25]	
0.4	2.066	2.053	2.014	2.014	1.955	1.956	2.066
0.6	2.039	2.030	1.981	1.985	1.921	1.921	2.045
0.8	2.038	2.028	1.976	1.977	1.905	1.904	2.046
1.25	2.061	2.059	1.991	1.990	1.899	1.898	2.084
10/6	2.110	2.107	2.021	2.019	1.909	1.906	2.141

† thickness as given in eqn (19)

The finite element results are gratifyingly close to the exact solution and/or the transfer matrix solution of Irie *et al.*[25].

In the nonlinear analysis, first a convergence study was conducted using two, four, and six elements (in half plate) of clamped circular plates. Table 5 shows a comparison of the present results for the ratio of nonlinear period to linear period (T_{NL}/T_L) with those obtained by Raju and Rao[38], who employed cubic elements based on the shear deformation theory. As can be seen from the table numerical convergence is good for all values of the amplitude-to-thickness ratio (c/t). The present SDT element converges from above while that of Raju and Rao[38] converges from below. Note that the classical plate theory predicts higher values of the ratio T_{NL}/T_L compared to the shear deformable theory.

Next, variable thickness circular plates were analyzed using the classical thin-plate theory. The thickness t is given by

$$t = t_1(1 - \alpha r/b) \tag{20}$$

where t_1 is the thickness at the center of the plate, and α is the taper parameter, $-1 < \alpha < 1$. For positive values of α the plate is tapered down toward the rim. Table 6 shows the ratio of the periods (T_{NL}/T_L) for various tapers of isotropic ($\nu = 0.3$) simply-supported and clamped plates.

Figure 9 shows the variation of the period ratio (T_{NL}/T_L) with respect to the amplitude-to-thickness ratio of variable thickness plates. As can be seen from the figure, the period ratio decreases with increasing c/t for fixed α and γ. Also, for fixed γ and c/t, the period decreases with increasing α. This is expected because the plate becomes thinner (toward the rim) with increasing α and hence vibrates at higher frequency (or smaller period). Finally, Fig. 10 shows similar results for free-clamped, variable thickness plates.

SUMMARY AND CONCLUSIONS

Motivated by the importance of the design data for variable-thickness annular plates, including the effects of shear deformation, large deflections, and material orthotropy, the present study was undertaken. The study employs the finite element method to solve the more

Table 5. Convergence study of the period ratio (T_{NL}/T_L) for isotropic ($\nu = 0.3$), uniform thickness clamped plate

a/t	c/t	Present Results (quadratic)			Raju and Rao [38](cubic)		
		2	4	6	2	4	8
SDT 5.0	0.0	1.0000	1.0000	1.0000	1.0000	1.0000	1.0000
	0.2	0.9923 (.9965)*	0.9922 (.9933)*	0.9921 (.9927)*	0.9919	0.9921	0.9921
	0.4	0.9704 (.9862)	0.9702 (.9741)	0.9702 (.9721)	0.9689	0.9696	0.9699
	0.6	0.9380 (.9699)	0.9374 (.9449)	0.9369 (.9411)	0.9339	0.9360	0.9366
	0.8	0.8990 (.9483)	0.8980 (.9093)	0.8978 (.9038)	0.8910	0.8954	0.8965
	1.0	0.8569 (.9225)	0.8550 (.8706)	0.8551 (.8629)	0.8438	0.8514	0.8533
CPT⁺	0.0	1.0000	1.0000	1.0000	1.0000	1.0000	1.0000
	0.2	0.9930	0.9928	0.9925	0.9930	0.9928	0.9928
	0.4	0.9730	0.9724	0.9722	0.9730	0.9724	0.9724
	0.6	0.9423	0.9413	0.9410	0.9423	0.9414	0.9413
	0.8	0.9040	0.9029	0.9027	0.9040	0.9030	0.9029
	1.0	0.8612	0.8605	0.8606	0.8613	0.8607	0.8607

* results obtained by using the linear element

⁺ Raju and Rao [38] obtained using a/t = 1000

Table 6. Ratio of the nonlinear period to linear period of isotropic ($\nu = 0.3$) simply supported and clamped plates for various values of the taper parameter† α and amplitude-to-thickness ratio, c/t.

α	c/t	simply-supported			clamped		
		2 elements	4 elements	6 elements	2 elements	4 elements	6 elements
0.1	0.2	0.9714	0.9714	0.9711	0.9919	0.9917	0.9919
	0.4	0.8995	0.8995	0.8989	0.9689	0.9685	0.9685
	0.6	0.8117	0.8113	0.8113	0.9341	0.9335	0.9336
	0.8	0.7256	0.7251	0.7249	0.8912	0.8910	0.8911
	1.0	0.6495	0.6490	0.6485	0.8441	0.8451	0.8452
0.3	0.2	0.9634	0.9633	0.9636	0.9886	0.9888	0.9888
	0.4	0.8764	0.8759	0.8754	0.9567	0.9575	0.9576
	0.6	0.7764	0.7755	0.7756	0.9100	0.9120	0.9121
	0.8	0.6848	0.6840	0.6841	0.8552	0.8593	0.8594
	1.0	0.6074	0.6065	0.6065	0.7977	0.8045	0.8048
0.5	0.2	0.9513	0.9505	0.9515	0.9823	0.9833	0.9833
	0.4	0.8442	0.8425	0.8436	0.9347	0.9382	0.9386
	0.6	0.7320	0.7304	0.7311	0.8694	0.8766	0.8774
	0.8	0.6367	0.6352	0.6359	0.7987	0.8094	0.8108
	1.0	0.5613	0.5585	0.5589	0.7299	0.7439	0.7459

† $t = t_1(1-\alpha r/b)$

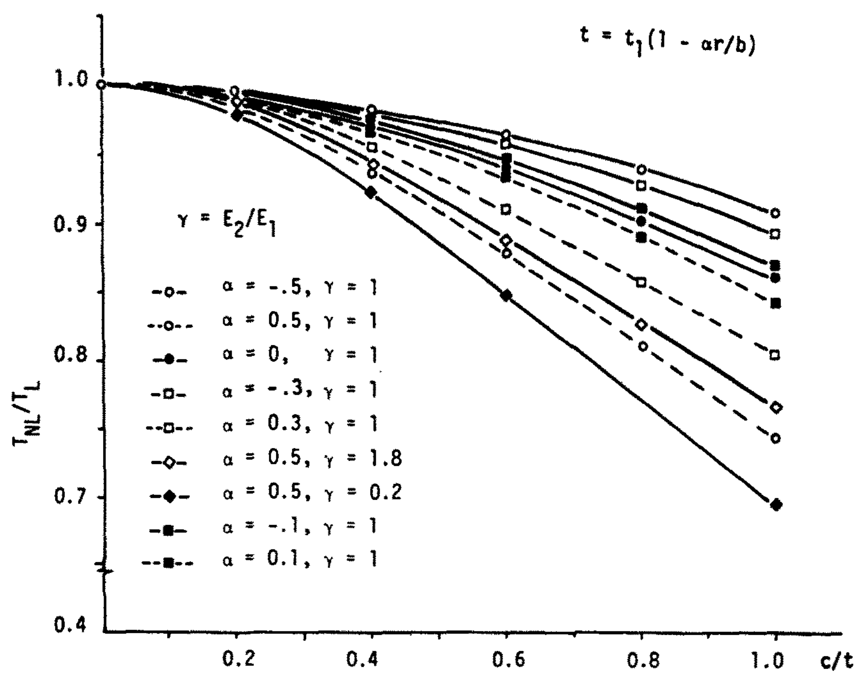

Fig. 9. Variation of T_{NL}/T_L with respect to the amplitude-to-thickness ratio of variable thickness clamped plate.

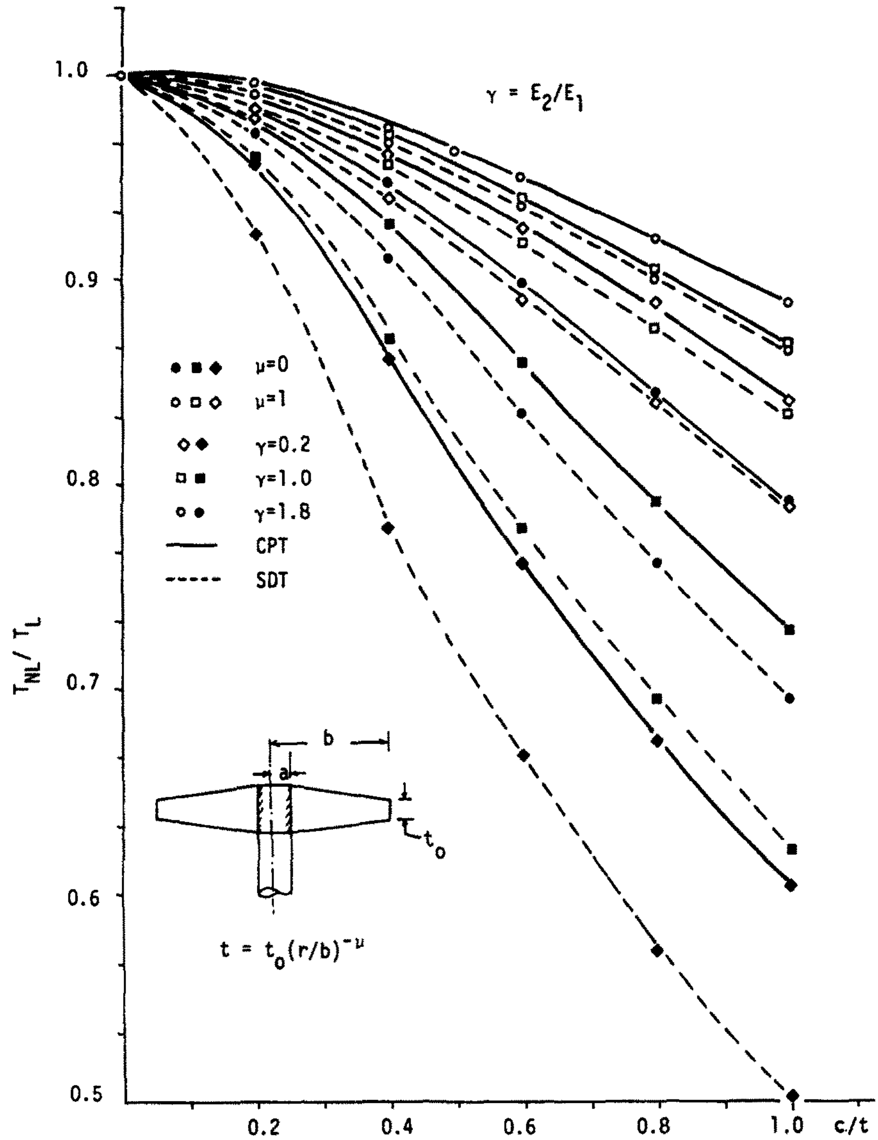

Fig. 10. Variation of T_{NL}/T_L with the amplitude-to-thickness ratio of free clamped variable thickness plates.

general Reissner plate equations as well as the von Karman plate equations for variable-thickness annular plates. Stresses and deformation results are presented showing the effects of radius-to-thickness ratio, inner radius-to-outer radius, nonlinearity, orthotropy and thickness profile. Free vibration analysis was performed and results of the ratio of nonlinear period to linear period are presented. The present finite element results are found to be in good agreement with available exact and approximate analytical solutions. Extension of the present study to transient analysis and unsymmetric bending is awaiting.

Acknowledgement—Support of this work by Structural Mechanics Program of the Office of Naval Research is gratefully acknowledged.

REFERENCES

1. A. M. Wahl and G. Lobo, Stresses and deflections in flat circular plates with central holes. *Trans. ASME* 52, 29–43 (1930).
2. R. D. Mindlin and H. Deresiewicz, Thickness shear and flexural vibrations of a circular disk. *J. Appl. Physics* 25, 1329–1332 (1954).
3. H. Deresiewicz and R. D. Mindlin, Axially symmetric flexural vibrations of a circular disk. *J. Appl. Mech.* 22, 86–88 (1955).

4. S. Timoshenko and S. Woinsky-Krieger, *Theory of Plates and Shells*. McGraw-Hill, New York (1959).
5. T. F. Lehnhoff and R. E. Miller, The influence of transverse shear on the small displacement theory of circular plates. *AIAA J.* **7**, 1499–1505 (1960).
6. G. J. Perakatte and T. F. Lehnhoff, Flexure of symmetrically loaded circular plates including the effect of transverse shear. *J. Appl. Mech.* **38**(4), 1036–1041 (1971).
7. S. Takahashi, K. Suzuki and Y. Nakamura, The vibrations of a circular plate with uniformly distributed load around the outer periphery. *Bulletin Japan Society of Mech. Engrs.* **16**, 714–723 (1973).
8. J. Kirkhope and G. J. Wilson, Vibration of circular and annular plates using finite elements. *Int. J. Numer. Meth. Engng.* **4**, 181–193 (1972).
9. G. C. Pardoen, Static, vibration and buckling analysis of axisymmetric circular plates using finite elements. *Computers Structures* **3**(2), 355–375 (1973).
10. S. S. Rao and A. S. Prasad, Vibrations of annular plates including the effects of rotory inertia and transverse shear deformation. *J. Sound Vibration* **42**, 305–324 (1975).
11. M. N. Bapu Rao and K. S. S. Kumaran, Finite element analysis of mindlin plates. *J. Mech. Design* **101**, 619–623 (1979).
12. H. D. Conway, The bending of symmetrically loaded circular plates of variable thickness. *J. Appl. Mech.* **15**(1), 1–6 (March 1948).
13. H. D. Conway, Note on the bending of curcular plates of variable thickness. *J. Appl. Mech.* **16**(2), 209–210 (June 1949).
14. H. D. Conway, Axially symmetrical plates with linearly variable thickness. *J. Appl. Mech.* **18**(2), 140–142 (June 1951).
15. H. D. Conway, Closed form solutions for plates by variable thickness *J. Appl. Mech.* **20**(4), 564–565 (Dec. 1953).
16. H. D. Conway, Non-axial bending of ring plates of varying thickness. *J. Appl. Mech.* **25**(3), 386–388 (1958).
17. P. H. W. Wolff, The design of flexible disk misalignment couplings. *Appl. Mech. Proc* The Institution of Mechanical Engineers, Vol. 165, pp. 165–175 (19751).
18. C. W. Bert, *Nonhomogeneous Polar-Orthotropic Circular Disks of Varying Thickness*. Engineering Experiment Station Bulletin, 190, The Ohio State University, Columbus (March 1962).
19. W. D. Pilkey, Stepped circular Kirchhoff plate. *AIAA J.* **3**(9), 1768–1770 (1965).
20. G. Z. Harris, The normal modes of a circular plate of variable thickness. *Q. J. Mech. and Appl. Mathematics* **21**, 321–327 (1968).
21. J. A. Gallego Juarez, Axisymmetric vibrations of circular plates with stepped thickness. *J. Sound Vibration* **26**, 411–416 (1973).
22. G. J. Wilson and J. Kirkhope, Vibration analysis of axial flow turbine disks using finite elements. *J. Engng. for Industry* **98**, 1008–1013 (1976).
23. G. J. Wilson and J. Kirkhope, Finite element bending analysis of nonuniform circular plates. *Computers Structures* **6**, 459–466 (1976).
24. T. Irie and G. Yamada, Analysis of free vibration of annular plate of variable thickness by the use of spline technique method. *Trans. Japan Soc. Mech. Engrs.* **45**, 681–688 (1979).
25. T. Irie, G. Yamada and S. Aomura, Free vibration of a mindlin annular plate of varying thickness. *J. Sound Vibration* **66**(2), 187–197 (1979).
26. G. F. Carrier, Stress distributions in cylindrically aeolotropic plates. *J. Appl. Mech., Trans. ASME* **10**, A117–A122 (1943).
27. G. F. Carrier, The bending of the cylindrically aeolotropic plate. *J. Appl. Mech., Trans. ASME* **11**(3), A129–A133 (Sept. 1944).
28. A. N. Sherbourne and D. N. S. Murthy. Elastic bending of anisotropic plates of variable thickness. *Int. J. Mech. Sci.* **12**, 1023–1035 (1970).
29. A. N. Sherbourne and D. N. S. Murthy, Bending of curcular plates with variable profile. *Computers Structures* **11**, 355–361 (1980).
30. V. G. Hart and D. J. Evans, Nonlinear bending of an annular plate by transverse edge forces, *J. Math. Phys.* **43**, 275–303 (1964).
31. W. E. Alzheimer and R. T. Davis, Nonlinear unsymmetrical bending of an annular plate. *J. Appl. Mech.* **35**, 190 (1968).
32. J. T. Tielking, Asixymmetric bending of annular plates. *J. Appl. Mech.* **45**(4), 834–838 (1978).
33. J. T. Tielking, Unsymmetric bending of annular plates. *Int. J. Solids Structures* **16**, 361–373 (1980).
34. T. Wah, Vibration of circular plates at large amplitudes. *J. Engng. Mech. Div., ASCE* **89**, (EM5), 1–15 (1963).
35. J. Ramachandran, Nonlinear vibrations of circular plates with linearly varying thickness. *J. Sound Vibration* **38**, 225–232 (1975).
36. Chu-Mie, Finite element displacement method for large amplitude free flexural vibrations of beams and plates. *J. Computers Structures* **3**, 163–174 (1973).
37. G. Venkateshwara Rao, K. Kanaka Raju and I. S. Raju, Finite element formulation for the large amplitude free vibrations of beams and orthotropic circular plates. *J. Computers Structures* **6**, 169–172 (1976).
38. K. Kanaka Raju and G. Venkateshwara Rao, Axisymmetric vibrations of circular plates including the effects of geometric non-linearity, shear deformation and rotory inertia. *J. Sound Vibration* **47**(2), 179–184 (1979).
39. G. Venkateshwara Rao and K. Kanaka Raju, Large amplitude axisymmetric vibrations of orthotropic circular plates elastically restrained against rotation. *J. Sound Vibration* **69**(2), 175–180 (1980).
40. J. N. Reddy, Simple finite elements with relaxed continuity for nonlinear analysis of plates. *Proc. 3rd Int. Conf. in Australia on Finite Element Methods*. pp. 265–281. University of New South Wales, Sydney (2–6 July 1979).
41. J. N. Reddy, A penalty plate-bending element for the analysis of laminated anisotropic composite plates. *Int. J. Num. Meth. Engng.* **15**, 1187–1206 (1980).
42. J. N. Reddy, C. L. Huang and I. R. Singh, Large deflections and large amplitude vibrations of axisymmetric circular plates. *Int. J. Num. Meth. Engng.* to appear (1981).
43. J. N. Reddy and I. R. Singh, Large deflections and large amplitude free vibrations of straight and curved beams. *Int. J. Num. Meth. Engng.* to appear (1981).